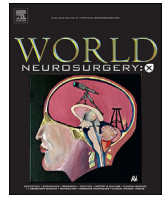


Contents lists available at [ScienceDirect](https://www.sciencedirect.com)

World Neurosurgery: X

journal homepage: www.journals.elsevier.com/world-neurosurgery-x

Differentiation of astrocytoma between grades II and III using a combination of methionine positron emission tomography and magnetic resonance spectroscopy

Hirohito Yano^{a,b,*}, Kazuhiro Miwa^c, Noriyuki Nakayama^d, Takashi Maruyama^e, Naoyuki Ohe^d, Soko Ikuta^e, Yuka Ikegame^{a,b}, Tetsuya Yamada^d, Hiroaki Takei^c, Etsuko Owashi^a, Kazufumi Ohmura^a, Kazutoshi Yokoyama^c, Morio Kumagai^a, Yoshihiro Muragaki^e, Toru Iwama^d, Jun Shinoda^{a,b}

^a Department of Neurosurgery and Chubu Medical Center for Prolonged Traumatic Brain Dysfunction, Chubu Neurorehabilitation Hospital, 630 Shimo-kobi, Kobi-cho, Minokamo, 505-0034, Japan

^b Department of Clinical Brain Science, Gifu University Graduate School of Medicine, 1-1 Yanagido, Gifu City, 501-1194, Japan

^c Department of Neurosurgery, Central Japan International Medical Center, 1-1 Kenkou-no-machi, Minokamo City, 505-8510, Japan

^d Department of Neurosurgery, Gifu University Graduate School of Medicine, 1-1 Yanagido, Gifu City, 501-1194, Japan

^e Department of Neurosurgery, Tokyo Women's Medical University, 8-1 Kawada-cho, Shinjuku-ku, Tokyo, 162-8666, Japan

ARTICLE INFO

Keywords:

Glioma
Grading
Isocitrate dehydrogenase
Magnetic resonance spectroscopy
Methionine
Positron emission tomography

ABSTRACT

Objective: This study aimed to establish a method for differentiating between grades II and III astrocytomas using preoperative imaging.

Methods: We retrospectively analyzed astrocytic tumors, including 18 grade II astrocytomas (isocitrate dehydrogenase (IDH)-mutant: IDH-wildtype = 8:10) and 56 grade III anaplastic astrocytomas (37:19). We recorded the maximum methionine (MET) uptake ratios (tumor-to-normal: T/N) on positron emission tomography (PET) and three MRS peak ratios: choline (Cho)/creatine (Cr), N-acetyl aspartate (NAA)/Cr, and Cho/NAA, between June 2015 and June 2020. We then evaluated the cut-off values to differentiate between grades II and III. We compared the grading results between contrast enhancement effects on MR and combinational diagnostic methods (CDM) on a scatter chart using the cutoff values of the T/N ratio and MRS parameters.

Results: The IDH-mutant group showed significant differences in the Cho/NAA ratio between grades II and III using univariate analysis; however, multiple regression analysis results negated this. The IDH-wildtype group showed no significant differences between the groups. Contrast enhancement effects also showed no significant differences in IDH status. Accordingly, regardless of the IDH status, no statistically independent factors differentiated between grades II and III. However, CDMs showed higher sensitivity and negative predictive value in distinguishing them than MRI contrast examinations for both IDH statuses. We demonstrated a significantly higher diagnostic rate of grade III than of grade II with CDM, which was more striking in the IDH-mutant group than in the wild-type group.

Conclusions: CDM could be valuable in differentiating between grade II and III astrocytic tumors.

Abbreviation: A-II, astrocytoma; A-III, anaplastic astrocytoma; AUC, area under the curve; CDM, combinational diagnostic method; Cho, choline; Cr, creatine; FOV, field of view; Gd, gadolinium; HGG, high-grade glioma; IDH, isocitrate dehydrogenase; LGG, low-grade glioma; MET, methionine; MRI, magnetic resonance imaging; MRS, magnetic resonance spectroscopy; NAA, N-acetyl aspartate; NPV, negative predictive value; PET, positron emission tomography; PPV, positive predictive value; ROC, Receiver operating characteristic; ROI, region of interest; SUV, standard uptake value; TE, echo time; TI, inversion time; T/N, tumor-to-normal frontal lobe; TR, repetition time; WI, weighted image.

* Corresponding author. Department of Neurosurgery and Chubu Medical Center for Prolonged Traumatic Brain Dysfunction, Chubu Neurorehabilitation Hospital, 630 Shimo-kobi, Kobi-cho, Minokamo, 505-0034, Japan.

E-mail address: hirohito@herb.ocn.ne.jp (H. Yano).

<https://doi.org/10.1016/j.wnsx.2023.100193>

Received 5 October 2022; Accepted 4 April 2023

2590-1397/© 2023 The Authors. Published by Elsevier Inc. This is an open access article under the CC BY-NC-ND license (<http://creativecommons.org/licenses/by-nc-nd/4.0/>).

1. Introduction

Since the adoption of the 2016 World Health Organization (WHO) classification,¹ we have come to call grade II/III gliomas lower-grade gliomas; however, a need to distinguish between high- and low-risk groups remains. Age, tumor size, contralateral infiltration, and neurological symptoms are the standard risk assessment parameters. However, metabolic markers in preoperative diagnostic imaging are clinically useful for an initial assessment.

Metabolic imaging of brain tumors includes methionine (MET)-positron emission tomography (PET) and magnetic resonance spectroscopy (MRS). MET-PET is reportedly helpful in glioma treatment by providing critical information, such as tumor grade^{2–6} and prediction of isocitrate dehydrogenase (IDH) status.^{6–10} In contrast, MRS provides essential metabolic information about N-acetyl aspartate (NAA), choline (Cho), and creatine (Cr) levels. Therefore, they can be used for tumor differentiation and grading.^{11–13}

IDH status and tumor grading are required to identify low- or high-risk individuals with lower-grade gliomas (grade II/III) at the preoperative stage for treatment and follow-up. Several studies have predicted IDH status using MET-PET,^{4,5,14} O-(2-18 F-fluoroethyl)-L-tyrosine (18 F-FET)-PET,¹⁵ magnetic resonance imaging (MRI),¹⁶ or 2-hydroxyglutarate on proton MRS.¹⁷ Although a number of studies have been conducted on MRS for glioma grading, they often aim to distinguish between low-grade glioma (LGG) and high-grade glioma (HGG).^{12,13,18} These analyses may depend mainly on the number of glioblastoma (GBM) cases. To the best of our knowledge, there has been only one report¹⁹ concerning the grading analysis of grade II and III astrocytic tumors using MRS.

Several studies have used MET-PET to grade gliomas. Some reports have shown a correlation between grades II and III^{3,5,6,9} or between grades III and IV.^{2,4} In other words, no report has demonstrated significant differences between grades II and III, and between grades III and IV in the same series. This may be due to the uneven distribution of grade III cases in both series. Therefore, there is no reliable parameter that can independently distinguish between grade II and III astrocytic tumors.

In this retrospective study, we attempted to differentiate between grade II and III astrocytomas using a combined diagnostic method (CDM) with standard MRS and MET-PET. Kudulaiti et al²⁰ reported¹¹ C-MET-PET/MRS combinational diagnoses for gliomas, in which they differentiated 95 non-enhancing gliomas from 14 non-tumors but did not differentiate between grade II and III gliomas in their method. Based on this metabolic information, we hypothesized that distinguishing between grades II and III would lead to risk evaluation. We also considered that this information would be enormously biased depending on the IDH status; therefore, we decided to distinguish between grades II and III based on the IDH status.

2. Patients and methods

Of the patients who underwent MET-PET and MRS on the same day at our institution between June 2015 and June 2020, we enrolled 74

primary lower-grade (II-III) astrocytic tumor patients diagnosed according to the 2016 WHO classification.¹ ATRX and TP53 immunohistochemistry supported the diagnosis of astrocytic tumors in addition to the findings of hematoxylin-eosin staining.

The number of patients in each group with the relevant clinical data is shown in Table 1. The median time from the PET/MRS examination to surgery was 42 days (3–462 days). IDH status was examined by immunohistochemistry using anti-IDH1 R132H and anti-IDH2 R172 antibodies, according to previously reported methods.⁴

Approval was granted by the Ethics Committee of the Kizawa Memorial Hospital (Minokamo City, Japan; approval no. 2021–001), the predecessor of the Central Japan International Medical Center (Minokamo City, Japan). The requirement for informed consent was waived due to the retrospective design of the study. We posted an information disclosure document on our hospital website (http://chubu-ryougo.jp/news/news/oshirase_220126.pdf) for patients who opted out.

2.1. PET

An Eminence STARGATE PET scanner equipped with a 3-dimensional acquisition system (Shimadzu Corporation, Kyoto, Japan) was used, which provided 99 transaxial images at 2.65-mm intervals. The in-plane spatial resolution full-width at half-maximum was 4.8 mm, and we scanned it in 3D mode. We injected a 3.5 MBq/kg MET dose intravenously via the cubital vein. Emission scans were acquired for 30 min, beginning 5 min after the MET injection. Tracer accumulation in the region of interest (ROI) was analyzed using standard uptake values (SUVs), defined as the active concentration in the ROI divided by the infusion volume, and normalized to the patient's body weight. The tumor-to-normal frontal lobe (T/N) ratio of the MET was calculated by dividing the maximum SUV of the tumor by the mean SUV of the contralateral normal frontal lobe, including the white and gray matter. We adopted the maximum tumor SUV to minimize the effect of tumor heterogeneity and the T/N ratio instead of the absolute SUV because of the high unexplained SUV variability. We performed co-registration of PET and MRI using the Dr. View software (AJS, Tokyo, Japan). The PET and MRI fusion images were defined as MET-PET images.

2.2. MRI

An Achieva 3.0 T TX QD MRI system (Philips, Amsterdam, Netherlands) was used to obtain transaxial T1-weighted images (WI) (repetition time/inversion time/echo time [TR/TI/TE] = 2200 ms/950 ms/9.5 ms, field of view [FOV] = 230 × 230 mm, matrix = 512 × 512) and T2-WI (TR/TE = 4000 ms/90 ms, FOV = 230 × 230 mm, matrix = 512 × 512). The slice thickness was 5 mm with a 1-mm slice gap. A 0.2 mL/kg body weight gadolinium-based contrast agent (Gd; Gadoteridol, Eisai, Japan) was intravenously injected. Three neurosurgeons determined the presence or absence of a contrast-enhanced tumor effect for each tumor grade without the patient's clinical and pathological information.

Table 1
Summary of cases.

	N	Age (Average ± SD)	male:female	Median days from PET/MRS to operation (range)
Astrocytoma (WHO grade II)				
IDH-mutant	8	40.4 ± 10.5	5:3	68.0 (20–462)
IDH-wildtype	10	50.9 ± 16.5	4:6	42.0 (9–154)
Anaplastic astrocytoma (WHO grade III)				
IDH-mutant	37	37.6 ± 12.2	18:19	40.0 (3–195)
IDH-wildtype	19	55.5 ± 14.9	12:7	42.5 (17–129)

PET = positron emission tomography, MRS = magnetic resonance spectroscopy, WHO=World Health Organization, IDH = isocitrate dehydrogenase.

2.3. MRS

Proton MRS was performed simultaneously with conventional MRI using a single-voxel point-resolved spectroscopy technique with TR/TE = 2000 ms/288 ms, which is the standard protocol for this MRI model. We manually placed a cubic voxel with a 2.0-cm side length on the lesion in which MET-PET showed the highest accumulation. The internal scanner software generated the spectra and provided automatic peak assignment and ratio calculations. Using Cr as the benchmark, we recorded the Cho/Cr, NAA/Cr, and Cho/NAA peak ratios. Using these parameters, the total acquisition time, including scanner adjustments, was <5 min.

2.4. Statistical analysis

We used the Mann–Whitney *U* test in R software (R Project for Statistical Computing, Vienna, Austria, version 4.0.3) to compare age, MRS parameters, and MET-T/N ratios between grades II and III. Multiple regression analysis was conducted to evaluate influential factors, including age, contrast enhancement on MRI, and WHO grade (II/III) for each ratio. Receiver operating characteristic (ROC) analysis using R software yielded the optimal threshold from the point where the sum of sensitivity and specificity was the highest on the ROC curve. Fisher's exact test was used to analyze the relationship between tumor grade and the Gd-enhancement effect, between tumor grade and classification by CDM, between Gd-enhancement effects and classification by CDM, and between tumor grade and the number of matched diagnostic items. Statistical significance was set at *P* < .05.

3. Results

3.1. MET-T/N ratio and MRS parameters in each glioma

Table 2 summarizes the NAA/Cr, Cho/Cr, Cho/NAA, and MET-T/N ratios for each tumor grade according to the IDH status. In the IDH-mutant group, only the Cho/NAA ratio differed significantly between grades II and III (*P* = .04). NAA/Cr, Cho/Cr, MET T/N ratio, and Gd enhancement were not significantly different between grades II and III. However, multiple regression analysis negated the significant correlation between WHO grade II/III and the Cho/NAA ratio (*p*-value of F

test = 0.11, Adjusted R-squared = 0.097, Supplementary data 1).

3.2. ROC analyses

In the IDH-mutant group, ROC curve analysis demonstrated an NAA/Cr ratio cut-off value of 0.65, with a sensitivity, specificity, and area under the curve (AUC) of 59.5%, 87.5%, and 0.711, respectively. Similarly, the cut-off values for Cho/Cr, Cho/NAA, and MET-T/N ratios were 2.61, 3.69, and 1.60, respectively (Table 3, Supplementary Fig. 1).

The cut-off values for the IDH-wildtype group for NAA/Cr, Cho/Cr, Cho/NAA, and MET-T/N ratios were 0.85, 2.07, 1.45, and 2.23, respectively (Table 3, Supplementary Fig. 1).

3.3. Differentiation between grade II/III astrocytomas

In the IDH-mutant group, the scatter chart was divided into two groups according to the MET-T/N and NAA/Cr ratios using each optimal threshold. Group A (MET-T/N ratio <1.60 and NAA/Cr ratio >0.65) and Group B (MET-T/N ratio ≥1.60 or NAA/Cr ratio ≤0.65) included seven cases of grade II and nine cases of grade III in Group A and one case of grade II and 28 cases of grade III in Group B (*P* = .002, Fig. 1A and B, Supplementary data 2). The scatter chart divided into Group C (MET-T/N ratio <1.60 and Cho/Cr ratio <2.61) and Group D (MET-T/N ratio ≥1.60 or Cho/Cr ratio ≥2.61) included all eight cases of grade II, 11 cases of grade III in Group C, and 26 cases of grade III in Group D (*P* = .0004, Fig. 1C and D; Supplementary data 2). The scatter chart divided into Group E (MET-T/N ratio <1.60 and Cho/NAA ratio <3.69) and Group F (MET-T/N ratio ≥1.60 or Cho/NAA ratio ≥3.69) included all eight cases of grade II and 10 cases of grade III in Group E and 27 cases of grade III in Group F (*P* = .0002, Fig. 1E, F, Supplementary data 2). Eleven cases with Gd enhancement were classified as grade III in the IDH mutant group. The numbers of cases with Gd enhancement in Groups B, D, and F were 10, 11, and 11, respectively. Group A included one case with Gd enhancement; however, Groups C and E included no cases with Gd enhancement (Group A vs. Group B: *P* = .07, Group C vs. Group D: *P* = .001, and Group E vs. Group F: *P* = .001, Supplementary data 3).

The scatter chart in the IDH-wildtype group was divided by the MET-T/N and NAA/Cr ratios into two windows, using each optimal threshold. Group G (MET-T/N ratio <2.23 and NAA/Cr ratio >0.85), Group H (MET-T/N ratio ≥2.23 or NAA/Cr ratio ≤0.85) showed a significant

Table 2
Results of MRS parameters and MET T/N ratio by IDH status.

	IDH-mutant			IDH-wildtype		
	Astrocytoma (grade II)	Anaplastic astrocytoma (grade III)	p value	Astrocytoma (grade II)	Anaplastic astrocytoma (grade III)	p value
Number of cases	8	37		10	19	
NAA/Cr ratio	1 ± 0.3	0.7 ± 0.4	0.07	1.0 ± 0.4	0.9 ± 0.6	0.41
Cho/Cr ratio	2.0 ± 0.3	2.6 ± 1.4	0.11	1.7 ± 0.6	1.9 ± 1.1	1.00
Cho/NAA ratio	2.2 ± 0.9	5.4 ± 4.8	0.04	2.1 ± 1.4	2.8 ± 2.3	0.42
MET T/N ratio	1.3 ± 0.2	1.8 ± 0.7	0.15	2.2 ± 0.8	2.6 ± 1.0	0.23
Gd-enhancement	0	11	0.17	4	6	0.70

MRS = magnetic resonance spectroscopy, MET = methionine, T/N = tumor-to-normal frontal cortex, IDH = isocitrate dehydrogenase, NAA=N-acetylaspartate, Cr = creatin, Cho = choline.

Table 3
Results of ROC analyses by IDH status.

	IDH-mutant				IDH-wildtype			
	NAA/Cr ratio	Cho/Cr ratio	Cho/NAA ratio	MET T/N ratio	NAA/Cr ratio	Cho/Cr ratio	Cho/NAA ratio	MET T/N ratio
Sensitivity (%)	59.5	48.6	48.6	43.2	63.2	36.8	78.9	63.2
Specificity (%)	87.5	100	100	100	60	80	50	80
Cut off value	0.65	2.61	3.69	1.60	0.85	2.07	1.45	2.23
AUC	0.71	0.68	0.74	0.67	0.60	0.50	0.60	0.64
95% CI	0.54–0.88	0.52–0.85	0.58–0.90	0.49–0.84	0.38–0.82	0.28–0.72	0.36–0.83	0.42–0.86

ROC = receiver operating characteristic, MET = methionine, T/N = tumor-to-normal frontal cortex, IDH = isocitrate dehydrogenase, NAA=N-acetylaspartate, Cr = creatin, Cho = choline, AUC = area under the curve, CI = confidence interval.

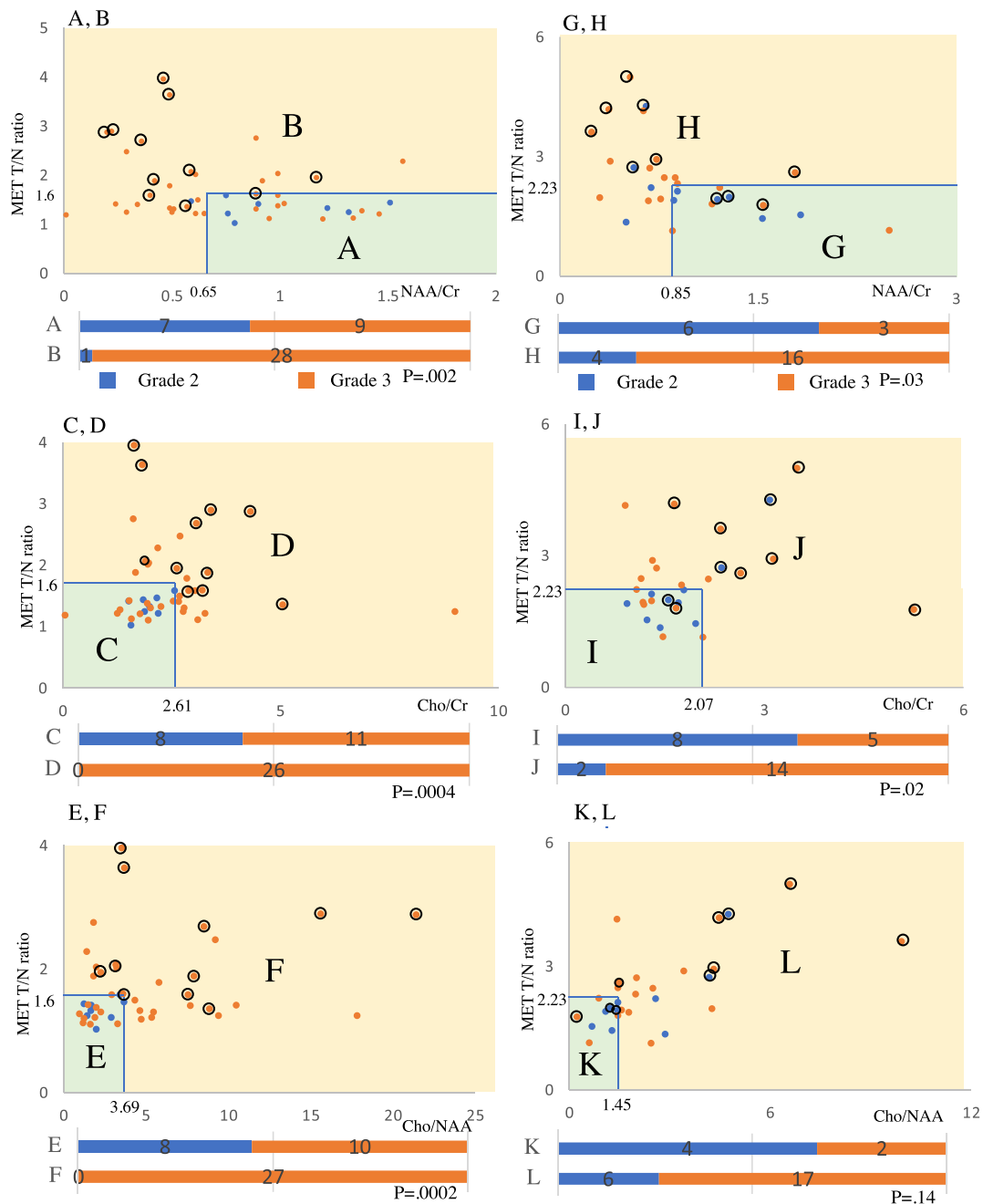


Fig. 1. Scatter charts showing the distribution of astrocytoma grade II (blue) and anaplastic astrocytoma grade III (orange) between the MET-T/N ratio and MRS parameters. The MRS parameters are the NAA/Cr ratio in [AB] and [GH], the Cho/Cr ratio in [CD] and [IJ], and the Cho/NAA ratio in [EF] and [KL]. The IDH-mutant cases are shown in [AB] [CD], and [EF], while those with IDH-wildtype are shown in [GH] [IJ], and [KL]. Groups A and G indicate areas over and below the threshold of the NAA/Cr and MET-T/N ratios, respectively. Groups C, E, I, and K indicate areas below the thresholds of both parameters. The numbers attached to the blue lines that divide the windows indicate the thresholds for each parameter. The open circles indicate the case with gadolinium enhancement effect. The bar graphs show the balance between grades II and III. The numbers in the graph indicate the number for each case.

difference between the distribution of Grade II and III cases ($P = .03$, Fig. 1G and H, Supplementary data 2). Similarly, the scatter chart divided into Group I (MET-T/N ratio <2.23 and Cho/Cr ratio <2.07) and Group J (MET-T/N ratio ≥ 2.23 or Cho/Cr ratio ≥ 2.07) showed a significant difference in distribution ($P = .02$, Fig. 1I and J, Supplementary data 2). Finally, only the scatter chart divided into Group K (MET-T/N ratio <2.23 and Cho/NAA ratio ≤ 1.45) and Group L (MET-T/N ratio ≥ 2.23 or Cho/NAA ratio ≥ 1.45) did not show a significant difference in distribution ($P = .14$, Fig. 1K, L, Supplementary data 2). Of the 10 cases with Gd-enhancement, four were grade II and six were grade III. The number

of cases with Gd enhancement in Groups H, J, and L were seven, eight, and seven, respectively. In contrast, Groups G, I, and K included three, two, and three cases, respectively (Group G vs. Group H: $P = 1$, Group I vs. Group J: $P = .11$, and Group K vs. Group L: $P = .67$, Supplementary data 3).

In a comparison of sensitivity, specificity, positive predictive value (PPV), negative predictive value (NPV), and accuracy between the CDM and Gd-enhancement, sensitivity and NPV were superior in all combination diagnoses compared with the Gd-enhancement method for both IDH statuses (Table 4, Supplementary data 2, 3).

Table 4
Comparison between combinational diagnosis and Gd-enhancement diagnosis for discriminating grade III from grade II in astrocytic tumors.

	MET T/N ratio and			Gd-enhancement
	NAA/Cr	Cho/Cr	Cho/NAA	
IDH-mutant				
sensitivity (%)	75.7	70.3	73	29.7
specificity (%)	87.5	100	100	100
PPV (%)	96.6	100	100	100
NPV (%)	43.8	42.1	44.4	23.5
accuracy (%)	77.8	75.6	77.8	42.2
IDH-wildtype				
sensitivity (%)	84.2	73.7	89.5	31.6
specificity (%)	60	80	40	60
PPV (%)	80	87.5	77.3	60
NPV (%)	66.7	61.5	71.4	31.6
accuracy (%)	75.9	75.9	72.4	41.4

MET = methionine, T/N = tumor to normal, NAA=N-acetylaspartate, Cr = creatin, Cho = choline, Gd = gadolinium, IDH = isocitrate dehydrogenase, PPV = positive predictive value, NPV = negative predictive value.

Next, we calculated the grade II and III ratios according to the number of matches in the judgment item based on IDH status (Fig. 2). We used four judgment items for the IDH-mutant group: MET-T/N ratio <1.6, NAA/Cr ratio >0.65, Cho/Cr ratio <2.61, and Cho/NAA ratio <3.69. When the number of matches of the judgment items was 0, 1, 2, 3, and 4, the diagnosis rates for grade II were 46.2%, 0%, 18.2%, 0%, and 0%, respectively ($P = .03$, Fig. 2). In contrast, in the IDH-wildtype group, we used four judgment items: MET-T/N ratio <2.23, NAA/Cr ratio >0.85, Cho/Cr ratio <2.07, and Cho/NAA ratio <1.45. When the number of matches of the judgment items was 0, 1, 2, 3, and 4, the diagnostic rates for grade II were 83.3%, 25.0%, 25.0%, 0%, and 40.0%, respectively ($P = .04$, Fig. 2). In both IDH statuses, the higher the number of matches of the judgment items, the significantly lower the rate of pathological diagnosis as grade II.

4. Discussion

Proton MRS provides important metabolic information concerning Cho, Cr, and NAA levels and the peak ratios of Cho/Cr, Cho/NAA, and NAA/Cr to characterize gliomas and the surrounding normal brain tissues. The Cho/NAA ratio is a proven sensitive parameter for detecting differences in tumor growth and is more reliable than the Cho/Cr ratio.²¹ Previous reports have revealed that higher Cho/NAA ratios were associated with a higher MIB-1 labeling index in HGG,²² while grade II gliomas reportedly showed no elevation of the Cho/Cr ratio⁷ and tended to show a higher NAA peak.⁸ Therefore, the Cho/NAA ratio will likely be a valuable parameter for diagnosing LGG. In our study, the CDM with Cho/NAA and MET T/N ratios showed the highest sum of sensitivity and specificity for distinguishing grades II and III in the IDH-mutant group.

In contrast, CDM by other combinations was not inferior to the combination of Cho/NAA and MET T/N ratio in the IDH-mutant group. Conversely, in IDH-wildtype astrocytomas, CDM was inferior in specificity, PPV, and accuracy of the CDM compared to those of the IDH-mutant group. Several reports have found significant differences between HGG and LGG using the Cho/NAA,¹¹ NAA/Cho,¹⁸ and Cho/Cr ratios.²³ In those studies, MRS analyses between LGG and HGG likely depended mainly on the specific characteristics of the GBM and the study population.²⁴ Only Möller-Hartmann et al¹⁹ reported a significant increase in the Cho/Cr ratio from low-grade astrocytoma to anaplastic astrocytoma to glioblastoma. In this study, there were no significant differences in the MRS parameters used to differentiate between grades II and III using multiple regression analysis. Therefore, MRS cannot independently distinguish between grades II and III.

However, whether the MET-T/N ratio can be used to distinguish grade II and III astrocytomas remains controversial. It was reported that the MET T/N ratio was as valuable as the SUV max in differentiating grades II and III.^{9,10} Aki et al³ and Nakajo et al⁵ reported a significant difference in the MET T/N ratios between A-II and A-III regardless of IDH status; however, Kato et al,² Takei et al,⁴ and Okita et al²⁵ did not report any such differences. Riva et al⁹ and Lopti et al¹⁰ reported that MET-PET

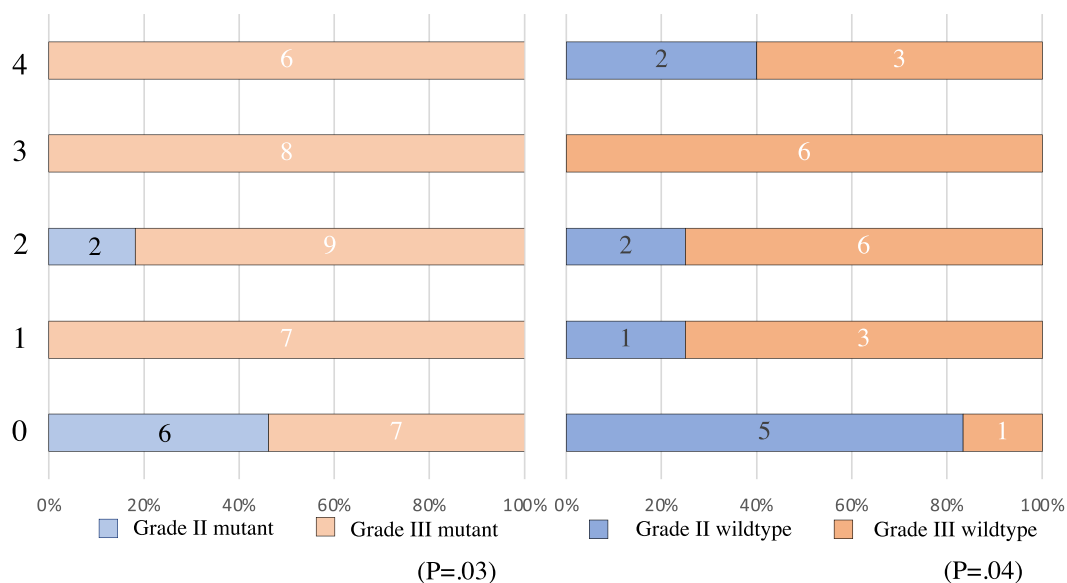


Fig. 2. The bar graphs indicate the balance of grades II and III by matching items out of the four. The numbers on the left side of the graph indicate the matching numbers of items. The numbers on the bars indicate the number for each case. Left: IDH-mutant group, for which the four diagnostic items are MET-T/N ratio <1.6, NAA/Cr ratio >0.65, Cho/Cr ratio <2.61, and Cho/NAA ratio <3.69. Right: IDH-wildtype group, for which the four diagnostic items were MET-T/N ratio <2.23, NAA/Cr ratio >0.85, Cho/Cr ratio <2.07, and Cho/NAA ratio <1.45.

was useful in differentiating grades II and III tumors, including oligodendroglial and astrocytic tumors. Only Kim et al⁶ reported a significant difference between A-II and A-III in the IDH-mutant group. The instability of these results was likely affected by the proportion of IDH status in each grade because SUV ratios were significantly higher in the IDH-wildtype.^{4-6,9,10} Therefore, investigation of IDH status was considered indispensable for grading astrocytomas regardless of IDH status. Unfortunately, Gd enhancement on MRI showed no significant difference between grades II and III in either IDH status groups. In particular, it is difficult to distinguish between non-enhanced grades II and III, for which we devised a CDM using the MET T/N ratio and MRS, including the NAA/Cr, Cho/Cr, and Cho/NAA ratios.

First, ROC analyses of the MET-T/N ratio and each MRS parameter were performed to obtain the best threshold for distinguishing A-III from A-II in each IDH status group. However, the AUC of all ROC curves was insufficient (Table 3), which was attributed to the fact that no factor independently showed a significant difference between A-II and A-III (Table 2).

Second, we created scatter charts for all the A-II and A-III cases using the MET-T/N ratio and one of the MRS parameters. Interestingly, Groups A, C, and E had a significantly higher number of A-II cases in the IDH-mutant group than in Groups B, D, and F (Fig. 1). Similarly, Groups G and I included a significantly larger number of A-II cases in the IDH-wildtype group than Groups H and J (Fig. 1). Accordingly, cases belonging to Groups B, D, F, H, and J were considered unlikely to be grade II. This tendency was more noticeable in the IDH-mutant group than in the IDH-wildtype group (Fig. 1).

All Gd-enhanced cases were grade III in the IDH-mutant group and belonged to Groups B, D, or F (Table 2, Fig. 1). Therefore, the numbers of non-enhanced cases belonging to Groups B, D, and F were 18, 15, and 16, respectively, of which all cases except one (Group B) were pathologically diagnosed as grade III in the mutant group. In contrast, in the wild-type group, the numbers of non-enhanced cases belonging to Groups H, J, and L were 13, 8, and 15, respectively, of which 11 (84.6%), 8 (100%), and 12 (80.0%) were pathologically diagnosed as grade III. Accordingly, we can diagnose non-enhanced cases belonging to Groups H, J, or L as grade II, with a probability of 20% or less.

Groups A, C, E, G, I, and K contained approximately half and half of the grade II and III cases, respectively. Although we could not separate these cases in these charts, it was assumed that there would be no striking difference in the biological activities based on the properties of each parameter. Considering the broad histological category of grade III, grade III cases in these areas may be histologically similar to grade II cases. Unfortunately, we did not confirm these findings histologically in this study.

Finally, we attempted the CDM using the four items mentioned above. Cases with three or more points could be reliably diagnosed as grade III in the mutant group, and it was better not to consider them as grade II. In the wild-type group, a grade II diagnosis was made in five of six cases (83.3%) with 0 points, in three of 12 cases (25%) with 1 or 2 points, and in two of 11 cases (18.3%) with 3 or 4 points. Therefore, the lower the points, the more statistically significant the cases of grade II for both IDH statuses. However, the fact that the CDM was inferior in the IDH-wildtype group compared to the IDH-mutant group suggests that the IDH-wildtype group contained biological malignancies beyond their histological findings. Significantly, CDM could be more beneficial for distinguishing between grades II and III in the IDH-mutant group than in the IDH-wildtype group.

The limitations of this study are the small number of cases and the large difference between the number of grade II and III cases owing to the retrospective nature of the study. Although we could not differentiate between grade II and III cases in one of the groups on the scatter charts, we need to observe their natural course to verify whether these cases correspond to a lower-risk group in future prospective studies. The WHO Classification of Tumors, 5th edition,²⁶ released in 2022, classifies all IDH-wildtype adult gliomas as grade 4 based on molecular testing, such

as telomerase reverse transcriptase promoter mutation, epidermal growth factor receptor amplification, and chromosome 7 gain/-chromosome 10 loss. We could not apply the CDM to the new classification because we did not perform these tests in this series. However, we believe that the CDM remains clinically useful for risk evaluation, at least for IDH-mutant astrocytoma.

5. Conclusions

The sensitivities, NPVs, and accuracies of the CDM were superior to those of the Gd-enhancement diagnoses in both IDH status groups (Table 4). In addition, the sensitivities in CDM were higher than those in the single diagnoses of MET-PET or MRS (Tables 3 and 4). Accordingly, CDM using MET-PET and MRS parameters was considered superior to MET-PET, MRS, and Gd-enhanced MRI alone. We believe that a grade diagnosis based on these two types of metabolic evaluation will be a meaningful reference for risk evaluation.

Credit author statement

Hirohito Yano: Conceptualization, Formal analysis, Validation, Writing-Original draft, preparation, **Kazuhiro Miwa:** Writing-review & editing, Formal analysis, **Noriyuki Nakayama:** Data curation, review & editing, **Takashi Maruyama:** review & editing, **Naoyuki Ohe:** Data curation, Investigation, **Soko Ikuta:** Data curation, Validation, **Yuka Ikegame:** Data curation, Validation, **Tetsuya Yamada:** Data curation, **Hiroaki Takei:** Investigation, **Etsuko Owashi:** Data curation, **Kazufumi Ohmura:** Data curation, **Kazutoshi Yokoyama:** Investigation, Project administration, **Morio Kumagai:** Data curation, Validation, **Yoshihiro Muragaki:** Supervision, **Toru Iwama:** Supervision, **Jun Shinoda:** Conceptualization, Supervision, writing-review & editing.

Funding

This research received no specific grants from public, commercial, or not-for-profit funding agencies.

Data availability statement

We will send the relevant documentation or data to verify the validity of the results upon request.

Code availability

Not applicable.

Ethics approval

All procedures were performed according to the ethical standards of the Institutional Committee and the 1964 Declaration of Helsinki and its later amendments or comparable ethical standards. Approval was granted by the Ethics Committee of the Kizawa Memorial Hospital (Minokamo City, Japan; approval no. 2021-001), the predecessor of the Central Japan International Medical Center (Minokamo City, Japan).

Consent to participate

This retrospective study was based on the secondary use of medical information. We waived individual informed consent. However, an information disclosure document was posted on our hospital website (http://chubu-ryougo.jp/news/news/oshirase_220126.pdf) to enable patients to opt-out.

Consent for publication

No consent is required for publication.

Declaration of competing interest

Dr. Toru Iwama received funding for research expenses unrelated to this study from Ogaki Tokushukai Hospital in 2020. The other authors declare no conflicts of interest.

Acknowledgments

We would like to thank the radiology staff of Chubu Medical Center for their technical support. We also thank the pathology staff of Tokyo Women's Medical University, Gifu University, and Kizawa Memorial Hospital for their histological and pathological expertise. Finally, we would like to thank Editage (www.editage.com) for the English language editing.

Appendix A. Supplementary data

Supplementary data to this article can be found online at <https://doi.org/10.1016/j.wnsx.2023.100193>.

References

- Louis DN, Ohgaki H, Wiestler OD, et al., eds. *WHO Classification of Tumours of the Central Nervous System*. 4th ed. Lyon, France: International Agency for Research on Cancer; 2016.
- Kato T, Shinoda J, Nakayama N, et al. Metabolic assessment of gliomas using 11C-methionine, [18F] fluorodeoxyglucose, and 11C-choline positron-emission tomography. *AJNR Am J Neuroradiol*. 2008;29:1176–1182. <https://doi.org/10.3174/ajnr.A1008>.
- Aki T, Nakayama N, Yonezawa S, et al. Evaluation of brain tumors using dynamic 11C-methionine-PET. *J Neuro Oncol*. 2012;109:115–122. <https://doi.org/10.1007/s11060-012-0873-9>.
- Takei H, Shinoda J, Ikuta S, et al. Usefulness of positron emission tomography for differentiating gliomas according to the 2016 World Health Organization classification of tumors of the central nervous system. *J Neurosurg*. 2019;133:1010–1019. <https://doi.org/10.3171/2019.5.JNS19780>.
- Nakajo K, Uda T, Kawashima T, et al. Diagnostic performance of [11C]methionine positron emission tomography in newly diagnosed and untreated glioma based on the revised World Health organization 2016 classification. *World Neurosurg*. 2021;148:e471–e481. <https://doi.org/10.1016/j.wneu.2021.01.012>.
- Kim D, Chun JH, Kim SH, et al. Re-evaluation of the diagnostic performance of 11C-methionine PET/CT according to the 2016 WHO classification of cerebral gliomas. *Eur J Nucl Med Mol Imag*. 2019;46:1678–1684. <https://doi.org/10.1007/s00259-019-04337-0>.
- Londoño A, Castillo M, Armao D, Kwock L, Suzuki K. Unusual MR spectroscopic imaging pattern of an astrocytoma: lack of elevated choline and high myo-inositol and glycine levels. *AJNR Am J Neuroradiol*. 2003;24:942–945.
- Nafe R, Herminghaus S, Raab P, et al. Preoperative proton-MR spectroscopy of gliomas—correlation with quantitative nuclear morphology in surgical specimen. *J Neuro Oncol*. 2003;63:233–245. <https://doi.org/10.1023/a:1024249232454>.
- Riva M, Lopci E, Castellano A, et al. Lower grade gliomas: relationships between metabolic and structural imaging with grading and molecular factors. *World Neurosurg*. 2019;126:e270–e280. <https://doi.org/10.1016/j.wneu.2019.02.031>.
- Lopci E, Riva M, Olivari L, et al. Prognostic value of molecular and imaging biomarkers in patients with supratentorial glioma. *Eur J Nucl Med Mol Imag*. 2017;44:1155–1164. <https://doi.org/10.1007/s00259-017-3618-3>.
- Bulik M, Jancalek R, Vanicek J, Skoch A, Mechl M. Potential of MR spectroscopy for assessment of glioma grading. *Clin Neurol Neurosurg*. 2013;115:146–153. <https://doi.org/10.1016/j.clineuro.2012.11.002>.
- Law M, Yang S, Wang H, et al. Glioma grading: sensitivity, specificity, and predictive values of perfusion MR imaging and proton MR spectroscopic imaging compared with conventional MR imaging. *AJNR Am J Neuroradiol*. 2003;24:1989–1998.
- Qi C, Li Y, Fan X, et al. A quantitative SVM approach potentially improves the accuracy of magnetic resonance spectroscopy in the preoperative evaluation of the grades of diffuse gliomas. *Neuroimage Clin*. 2019;23, 101835. <https://doi.org/10.1016/j.nicl.2019.101835>.
- Zhou W, Zhou Z, Wen J, et al. A nomogram modeling 11C-MET PET/CT and clinical features in glioma helps predict IDH mutation. *Front Oncol*. 2020;10:1200. <https://doi.org/10.3389/fonc.2020.01200>.
- Verger A, Stoffels G, Bauer EK, et al. Static and dynamic 18F-FET PET for the characterization of gliomas defined by IDH and 1p/19q status. *Eur J Nucl Med Mol Imag*. 2018;45:443–451. <https://doi.org/10.1007/s00259-017-3846-6>.
- Park YW, Han K, Ahn SS, et al. Prediction of IDH1-mutation and 1p/19q-codeletion status using preoperative MR imaging phenotypes in lower grade gliomas. *AJNR Am J Neuroradiol*. 2018;39:37–42. <https://doi.org/10.3174/ajnr.A5421>.
- Suh CH, Kim HS, Jung SC, Choi CG, Kim SJ. 2-Hydroxyglutarate MR spectroscopy for prediction of isocitrate dehydrogenase mutant glioma: a systemic review and meta-analysis using individual patient data. *Neuro Oncol*. 2018;20:1573–1583. <https://doi.org/10.1093/neuonc/noy113>.
- Harada M, Tanouchi M, Nishitani H, Miyoshi H, Bandou K, Kannuki S. Non-invasive characterization of brain tumor by in-vivo proton magnetic resonance spectroscopy. *Jpn J Cancer Res*. 1995;86:329–332. <https://doi.org/10.1111/j.1349-7006.1995.tb03059.x>.
- Möller-Hartmann W, Herminghaus S, Krings T, et al. Clinical application of proton magnetic resonance spectroscopy in the diagnosis of intracranial mass lesions. *Neuroradiology*. 2002;44:371–381. <https://doi.org/10.1007/s00234-001-0760-0>.
- Kudulaiti N, Qiu T, Lu J, et al. Combination of magnetic resonance spectroscopy and ¹¹C-methionine positron emission tomography for the accurate diagnosis of non-enhancing supratentorial glioma. *Korean J Radiol*. 2019;20:967–975. <https://doi.org/10.3348/kjr.2018.0690>.
- McKnight TR, Lamborn KR, Love TD, et al. Correlation of magnetic resonance spectroscopic and growth characteristics within Grades II and III gliomas. *J Neurosurg*. 2007;106:660–666. <https://doi.org/10.3171/jns.2007.106.4.660>.
- Chen J, Huang SL, Li T, Chen XL. In vivo research in astrocytoma cell proliferation with 1H-magnetic resonance spectroscopy: correlation with histopathology and immunohistochemistry. *Neuroradiology*. 2006;48:312–318. <https://doi.org/10.1007/s00234-006-0066-3>.
- Likavcanová K, Dobrota D, Liptaj T, et al. In vitro study of astrocytic tumour metabolism by proton magnetic resonance spectroscopy. *Gen Physiol Biophys*. 2005;24:327–335.
- Delgado AF, Delgado AF. Discrimination between glioma grades II and III using dynamic susceptibility perfusion MRI: a meta-analysis. *AJNR Am J Neuroradiol*. 2017;38:1348–1355. <https://doi.org/10.3174/ajnr.A5218>.
- Okita Y, Shofuda T, Kanematsu D, et al. The association between 11C-methionine uptake, IDH gene mutation, and MGMT promoter methylation in patients with grade II and III gliomas. *Clin Radiol*. 2020;75:622–628. <https://doi.org/10.1016/j.crad.2020.03.033>.
- The WHO Classification of Tumours Editorial Board. In: *WHO Classification of Tumours*. Lyon: International Agency for Research on Cancer; 2022:Central Nervous System Tumours. 5th ed.